Scanning Microscopy

Volume 7 | Number 1 Article 3

10-28-1992

Microanalysis of Individual Silver Halide Microcrystals

Shijian Wu
University of Antwerp

A. Van Daele
University of Antwerp

W. Jacob
University of Antwerp

R. Gijbels
University of Antwerp

A. Verbeeck
Agfa-Gevaert

See next page for additional authors

Microanalysis of Individual Silver Halide Microcrystals

Authors

Shijian Wu, A. Van Daele, W. Jacob, R. Gijbels, A. Verbeeck, and R. De Keyzer

Scanning Microscopy, Vol. 7, No. 1, 1993 (Pages 17-24)
Scanning Microscopy International, Chicago (AMF O'Hare), IL 60666 USA

0891-7035/93$5.00+.00

MICROANALYSIS OF INDIVIDUAL SILVER HALIDE MICROCRYSTALS

Shijian Wu[1,*], A.Van Daele[2], W.Jacob[2], R.Gijbels[1], A. Verbeeck[3], and R. De Keyzer[3]

[1]Departments of Chemistry and [2]Medicine, University of Antwerp (U.I.A)
Universiteitsplein 1, B-2610, Wilrijk, Belgium.
[3]Agfa-Gevaert N.V., B-2640, Mortsel, Belgium.

(Received for publication May 5, 1992, and in revised form October 28, 1992)

Abstract

Elemental distributions and contents of tabular and cubic silver halide microcrystals were analyzed by backscattered electron imaging, scanning transmission electron imaging, X-ray mapping and X-ray analysis in the spot mode by scanning transmission electron microscopy (STEM) combined with energy-dispersive X-ray spectrometry (EDXS). By using a liquid nitrogen cryostage, damage to the microcrystals and drift of the sample under electron bombardment were minimized. Monte Carlo simulation shows the electron trajectories in the silver halide microcrystals for different experimental conditions and directs the selection of the beam position for X-ray spot analysis. The backscattered electron images, scanning transmission electron images and X-ray maps were acquired after selecting the optimal operation parameters of the image processing system. The quality of backscattered electron images was improved by processing the images off line. The X-ray maps directly show the elemental distribution in individual microcrystals, the backscattered electron images and the scanning transmission electron images do so indirectly. X-ray analyses in the spot mode yield semiquantitative results. This work indicates that the combination of the different modes can be used to assess elemental distribution and content in the microcrystals, even cubic ones.

Key Words: Silver halide photographic microcrystal, backscattered electron image, scanning transmission electron image, X-ray mapping, X-ray microanalysis, Monte Carlo calculations.

*Address for correspondence:
R. Gijbels
Dept. of Chemistry, University of Antwerp (U.I.A)
Universiteitsplein 1
B-2610 Wilrijk, Belgium
Telephone number: 32-3-8202382

Introduction

In order to improve the photographic properties of silver halide emulsions, various preparation methods have been developed for controlling the shape, size, composition and halide distribution. Different types of silver halide microcrystals have been investigated in recent years, such as core-shell emulsions, twinned tabular grains, and microcrystals with epitaxial and conversion growths. Since the composition and the elemental distribution of silver halide microcrystals have an important effect on the photographic properties, these studies are being pursued with continued interest, particularly for individual microcrystals. X-ray photoelectron spectroscopy (Kelly and Mason, 1976) can be used to determine the composition of the surface of silver halides, the composition of individual microcrystals can be studied by analytical electron microscopy (King *et al.*, 1987), compositional depth profiles of populations of microcrystals can be derived with secondary ion mass spectrometry (SIMS) (Gijbels *et al.*, 1987), the application of scanning SIMS can yield the compositional image of some microcrystals (Maternaghan *et al.*, 1990), low temperature luminescence microscopy can show the iodide distribution in case of a low concentration of iodide in the tabular silver iodobromide grains (Maskasky, 1987). In spite of these studies, a lot of work remains to be done on the microstructure of silver halides, particularly on the microanalysis of individual microcrystals. Of these techniques, only analytical electron microscopy can provide direct observation and microanalysis of individual microcrystals.

In previous work we studied the distributions and contents of halides in tabular microcrystals by using backscattered electron imaging (BSEI) and by X-ray mapping and analysis in the spot mode (Gao *et al.*, 1989; Wu *et al.*, 1990). Because tabular microcrystals are flat, their analysis can be carried out relatively easily compared to other shaped grains. For microcrystals of other shapes, the analysis needs to be improved and further developed. Obviously, the combination of a series of analytical techniques can provide more effective and quantitative information. In the present work, we studied the halide distribution in tabular silver halide

microcrystals with epitaxial growths, in cubic silver halide microcrystals with AgBr epitaxial growths at the corners and with bromide conversion, and in cubic core-shell emulsions with AgCl core and Ag(Cl, Br) shell, using scanning transmission electron microscopy with energy-dispersive X-ray spectrometry (STEM-EDXS).

Basic Theory

Estimation of primary electron scattering in silver halide microcrystals

By simulating electron scattering events in the target volume, Monte Carlo electron trajectory calculations can provide a powerful means for the study of the characteristics and distributions of the various signals generated in electron-specimen interactions. This effectively defines the spatial resolution of an X-ray analysis in the sample. Details of the Monte Carlo electron trajectory simulation methods can be found in the literature (Newbury and Yakowitz, 1976; Joy, 1988).

The programs were provided by D.C. Joy and were implemented on an IBM-PC personal computer. They can simulate various experimental conditions such as single electron scattering in thin or bulk samples, X-ray production in thin films and depth variation, and so on.

The parameters necessary for calculating single scattering Monte Carlo trajectory simulation are the following: **1**) accelerating voltage; **2**) density of target; **3**) mean atomic number; **4**) mean atomic weight; **5**) electron beam size; **6**) thickness of the target; **7**) number of trajectories. For AgBr, the mean atomic number is 41, the density is 6.475 g/cm^3 and the mean atomic weight is 93.89. For AgCl, the mean atomic number is 32, the density is 5.567 g/cm^3 and the mean atomic weight 71.66. Figures 1a and 1b respectively show Monte Carlo simulations of 100 trajectories with a 5 nm electron probe size and the depth distribution of X-ray production with a zero beam diameter electron probe in a tabular silver bromide microcrystal of 0.1 μm thickness at 80 keV primary electron energy. Figures 2a and 2b respectively show Monte Carlo simulations of 100 trajectories with a 5 nm electron probe and the depth distribution of X-ray production with a zero beam diameter electron probe size in a cubic silver chloride microcrystal of 0.5 μm thickness at 80 keV primary electron energy.

The Backscattering Coefficient

The electron backscattering depends on the atomic number. Various models for electron backscattering are reported in the literature. For example, Niedrig (1978) combined the equation proposed by Everhart (1960) for single Rutherford scattering with an isotropic diffusion term as used by Archard (1961). This theory is in good agreement with experimental data. Expressions have been described for calculating the backscattering coefficient in the case of a thin, unsupported film (see for instance, Raeymaekers *et al.*, 1986).

In silver halide analysis, the microcrystals are supported with a carbon coated grid. The composition of the carbon film is homogeneous, the atomic number is low compared to that of silver halides, and the film is very thin. The influence of the substrate on the backscattering coefficient can be neglected. Thus, the electron backscattering coefficient is a function of the average atomic number, the average atomic mass, the density, the specimen thickness and the initial electron energy. The latter is constant under given experimental conditions. For a silver halide microcrystal of a given thickness, the differences in the electron backscattering coefficient are related to the differences in average atomic number, thus, the backscattered electron imaging can show compositional contrast in a silver halide microcrystal of uniform thickness.

Experimental

Different kinds of silver halide microcrystals were prepared. After removing the gelatin of the silver halide emulsion, repeated centrifugation and washing in distilled water, the grains were resuspended in butanol and dispersed onto carbon coated 50 mesh copper grids. All analyses were carried out on a JEOL JEM-1200 EX-TEMSCAN electron microscope equipped with an integrated scanning device EM-ASID10, an annular semiconductor BSE detector and a 30 mm^2 Si(Li) energy-dispersive X-ray detector and multichannel analyzer [Tracor Northern (TN) 5500]. A KONTRON IBAS image processing system (IPS) with an INTEL 80286 based host control processor was used for acquiring and processing secondary electron images, backscattered electron images and elemental X-ray maps. The role of the image processing computer system is twofold: it allows us to optimize the acquisition conditions and to process the images afterwards. For different scanning modes (SE, BSE, scanning transmission electron STE, X-ray map), different programs were used. After inputting a series of optimum acquisition parameters such as the dwell time per pixel, frame loops, total number of pixels, and a window of analysis, the computer hardware takes control over the scanning system of the microscope. This makes it easy to get images with high signal to noise ratio. In addition, the images can be stored in the processing system and processed off line, which obviously enables the analysis time at the electron microscope to be decreased. Image processing can be performed so as to enhance the contrast of the image and see more details. Background subtraction of X-ray maps can also be performed in the IPS.

The measurements were carried out at 80 kV accelerating voltage, with magnifications of 20,000 to 100,000 times depending on the specimens. This range of magnifications corresponded to electron probe sizes of about 10 nm to 2 nm. It is worth noting at this point that for imaging in the SE, BSE, and STE modes, the sample is horizontal (see Fig. 3), but for X-rays measurements, the sample is tilted 35° to 40° relative to the

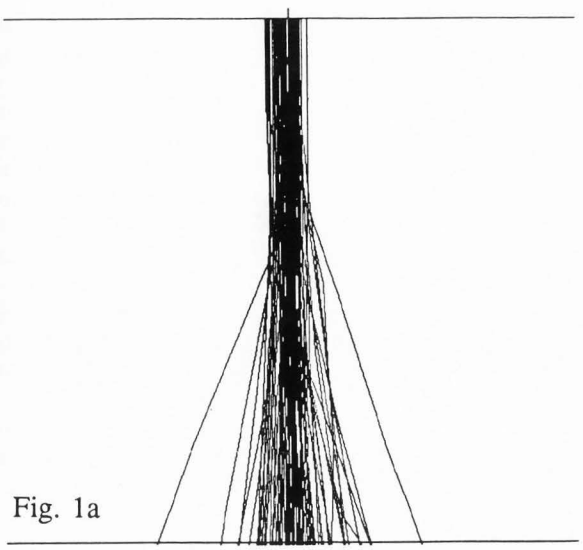

Fig. 1a

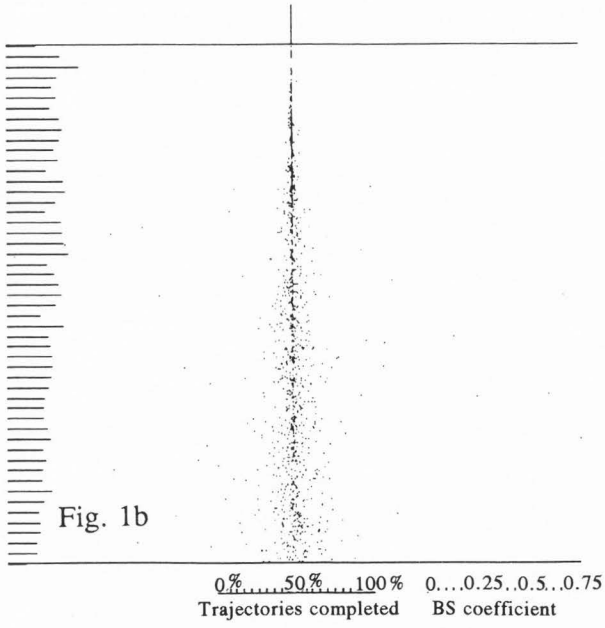

Fig. 1b

Figure 1. (**a**) Electron distribution simulated by Monte Carlo calculation in AgBr with 0.1 μm thickness at 80 keV primary electron energy with 5 nm electron probe size, 100 trajectories; (**b**) Generation and depth distribution of AgLα in AgBr with 0.1 μm thickness at 80 keV incident energy with a zero beam diameter electron probe, 500 trajectories. The length of the bars at the left shows the relative value of $\phi(\rho z)$ at that depth.

---

horizontal (see Fig. 4). X-rays were acquired by the TN 5500 analyzer with energy window widths set at 2 times full width at half maximum (FWHM). The X-ray analysis was done in the spot mode for a live time of typically 100 seconds.

A liquid nitrogen cryostage (Gatan Model 636 double tilt cooling holder) was used to minimize sample

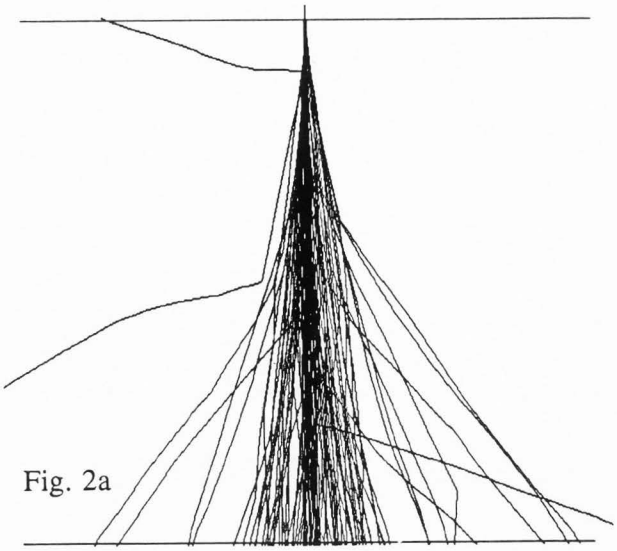

Fig. 2a

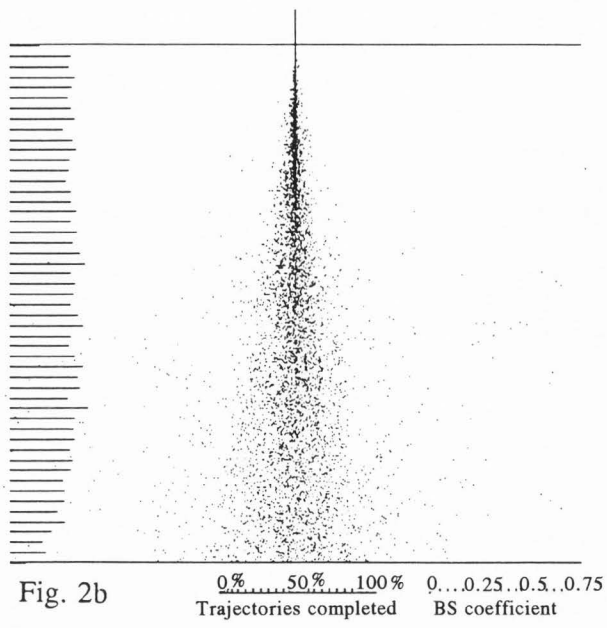

Fig. 2b

Figure 2. (**a**) Electron distribution simulated by Monte Carlo calculation in AgCl with 0.5 μm thickness at 80 keV primary electron energy with 5 nm electron probe size, 100 trajectories; (**b**) Generation and depth distribution of AgLα in AgCl with 0.5 μm thickness at 80 keV incident energy with a zero beam diameter electron probe, 500 trajectories.

---

damage and drift under electron bombardment. The temperature of the specimen was kept at 106 °K. At this temperature, experiments showed that the X-ray count rates for the elements in silver halide can be considered as constant in the X-ray spot analysis mode; this conclusion was reached by comparing counts of the first 100 second dwell time and those of the tenth 100 second dwell time.

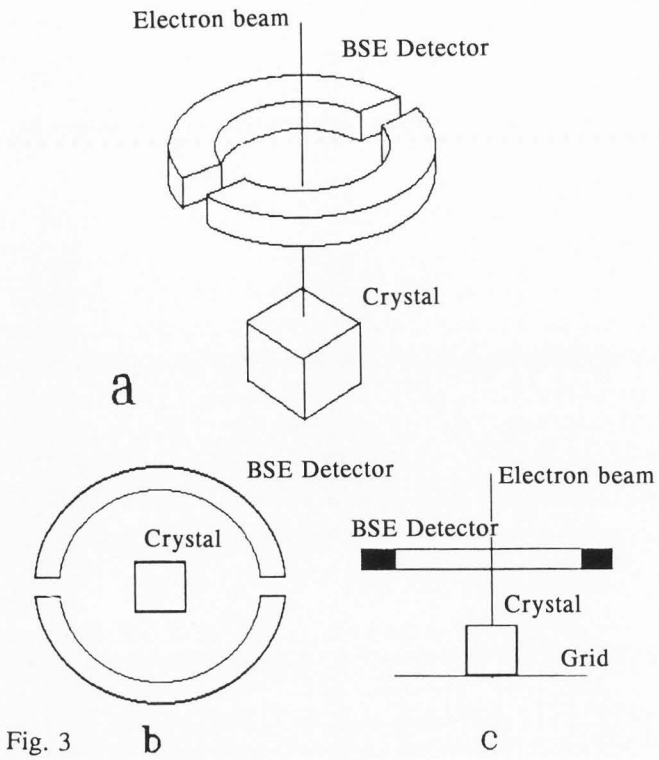

Fig. 3

Figure 3. Schematic representation of a cubic silver halide microcrystal in horizontal position for the acquisition of SE, BSE and STE images. (**a**) outline of the position of the BSE detector and a microcrystal; (**b**) vertical view (seen along the electron beam); (**c**) side view (perpendicular to the plane defined by electron beam and axis of X-ray detector).

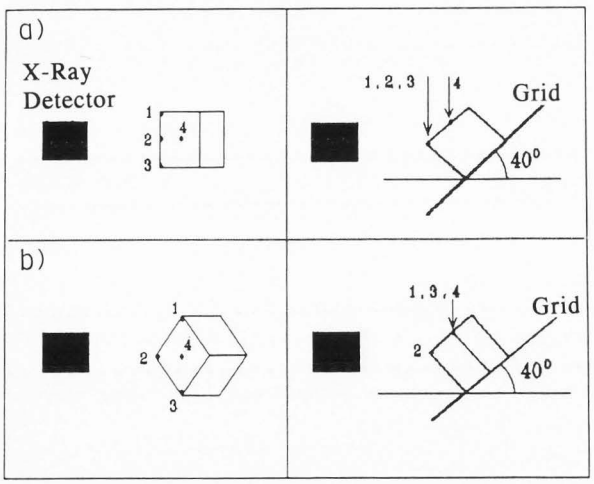

Figure 4. Schematic representation of two orientations (**a** and **b**) of silver halide microcrystals tilted 40° relative to the horizontal position for the acquisition of the X-ray spectra, left: vertical view (seen from above along the electron beam); right: side view (arrows indicate incoming electron beam). The height of the crystal is 2 μm.

Monte Carlo electron trajectory simulations in tabular silver bromide microcrystals (Fig. 1a) and cubic silver chloride microcrystals (Fig. 2a) show the primary electron scattering and also show the spatial resolution of X-ray analysis in the two types of silver halide microcrystals (Figures 1b and 2b); it appears that because of primary radiation penetration and broadening within the microcrystal, the X-rays are produced within a much larger and less well defined volume than the electron probe size; also the lateral diffusion of secondary electrons increases with the thickness of the silver halide microcrystal. Sample tilting of 35° and 40° respectively is used for X-ray mapping and for X-ray analysis in the spot mode. Because of this, the image of the microcrystals is distorted. For tabular microcrystals, the analysis position in the X-ray spot mode can directly be selected in a straightforward way as needed. However, the situation is different for cubic microcrystals: the selection of the analysis spot must take into account the penetration and broadening of the electron beam, for a given orientation of the crystal and for a given site in or on the crystal (corner, side, center, etc.). This is illustrated in Fig. 4.

Results and Discussions

Monte Carlo models calculate the interaction of the primary electron beam with specimen material and describe scattering events that determine the electron paths. For tabular AgBr microcrystals having a thickness of 0.1 μm (Fig. 1a), the calculation shows that beam broadening is limited: starting with a 5 nm primary beam, it is found that the beam broadening range, the diameter within which 90% of the transmitted electrons lie, is within a diameter of 9 nm and that most electrons penetrate the microcrystal. This indicates that the influence of primary beam broadening to neighbouring parts is relatively small and therefore BSE image, TE image, and X-ray map can show high lateral resolution. For a cubic microcrystal, the beam broadening becomes more significant, the broadening range in AgCl (thickness 0.5 μm) is 147 nm and in AgBr (thickness 0.5 μm) it is 243 nm. The primary electron beam broadening results in poor resolution of the electron images and an increase of the X-ray excitation volume, this suggests that, as would be expected, the influence of the primary electron beam on the surroundings must be recognized and the analytical uncertainty should be reckoned with in the X-ray analysis of cubic microcrystals. When directing the electron beam to positions 1, 2, 3 of a microcrystal (Figures 4a and 4b), the sampled volume is much smaller, and the lateral resolution should therefore be considerably better.

The processed BSE image of a hexagonal tabular AgBr microcrystal with Ag(Br,I) epitaxial growths is shown in Fig. 5a. As said above, BSE image can show composition contrast. We can calculate that the average atomic number $Z_{(AgI)}$ is 50, $Z_{(AgBr)}$ is 41 and $Z_{(AgCl)}$ is 32. Hence, the brighter part in the BSE image (Fig. 5a) indicates a high iodide concentration in the Ag(Br,I)

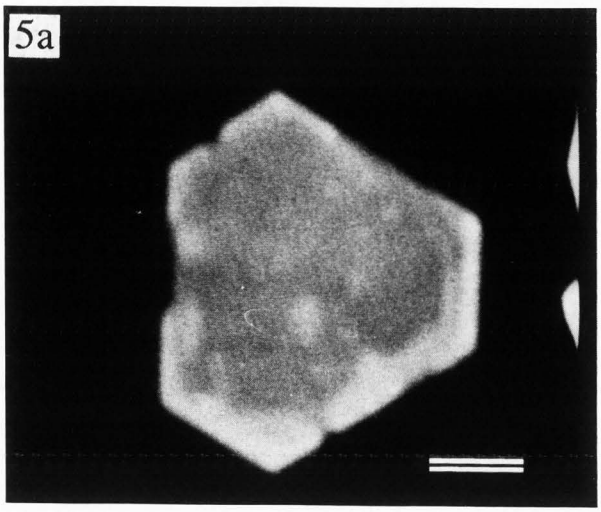

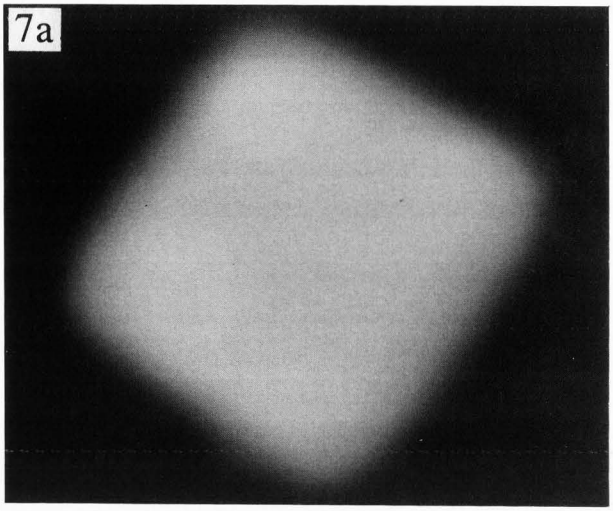

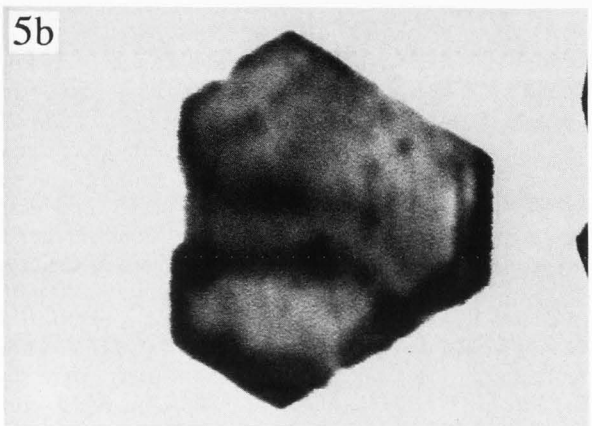

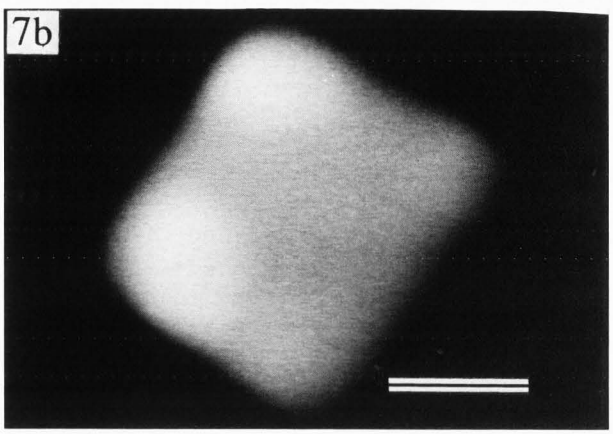

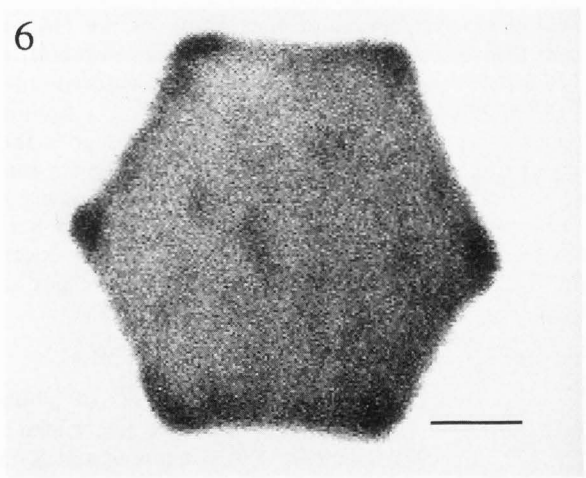

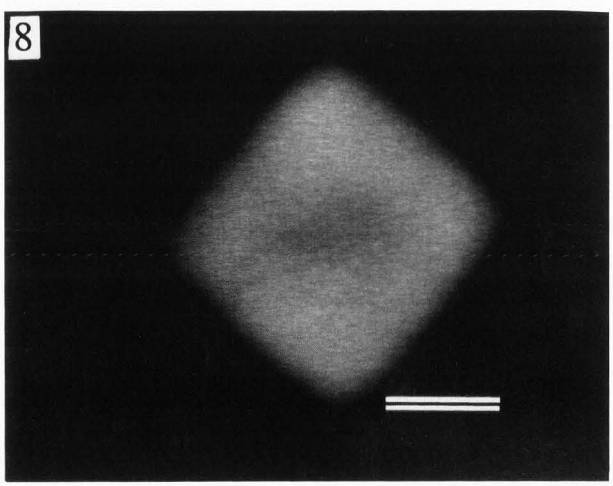

Figure 5. BSE (**a**) and STE (**b**) images of a tabular AgBr microcrystal with Ag(Br,I) epitaxial growths. Bar = 0.5 μm.

Figure 6. STE image of a tabular AgBr microcrystal with Ag(Br,I) epitaxial growths inside the corners. Bar = 0.5 μm.

Figure 7. BSE image of a cubic AgCl microcrystal with AgBr epitaxial growths in the corners. (**a**) before image processing; (**b**) after image processing. Bar = 0.2 μm.

Figure 8. Processed BSE image of a cubic AgCl core-Ag(Cl,Br) shell microcrystal. Bar = 0.2 μm.

microcrystal. The images show clearly that the epitaxial growth occurs at the corners of the tabular silver halide microcrystals or at the surface of the microcrystals. Fig. 5b shows the STE image of this tabular microcrystal. Compared to the Fig. 5a, Fig. 5b shows opposite signal intensity, but similar characteristics. The resolution of the STE image is better than that of the BSE image. The STE signal is stronger than the BSE signal, and the image does not need to be processed. In the STE image, the image contrast is due to the electron and mass density difference. These depend on the difference of average atomic number and mass, so it can be used to show the elemental distribution. Fig. 6 shows an example of a STE image where the Ag(Br,I) epitaxial parts grew inside the corners of the microcrystal. Semiquantitative analysis results were obtained by EDXS spot analysis. This confirmed that the darker parts in STEI (Fig. 5b) and the brighter parts in BSEI correspond to high iodide concentration and that the STE image can also clearly show the iodide distribution.

Elemental distributions of cubic Ag(Cl,Br) microcrystals were determined by backscattered electron imaging, X-ray mapping and X-ray analysis in the spot mode. The compositional contrast of processed BSE images corresponded with the elemental maps of some samples. Fig. 7a shows a BSE image acquired directly from the electron microscope after selecting the optimum parameters of IPS operation. Fig. 7b shows the BSE image processed by IPS, and indeed, the contrast of the BSE image of the cubic microcrystal can be increased after digital image processing as can be seen by comparing Figures 7a and 7b. Fig. 7b points to high bromide concentration at the corners and shows that the growth at the corners was on the inside of the cubic microcrystals.

For the AgCl core-Ag(Cl,Br) shell microcrystals with the same structure but different bromide concentration, BSE images also show qualitative results. Fig. 8 is the processed BSE image of the microcrystals with an AgCl core and 20% bromide in the Ag(Cl,Br) shell. The BSE micrograph taken directly from the electron microscope screen did not show the halide distribution in these core-shell microcrystals, the use of the IPS allowed to enhance the compositional contrast sufficiently to show the double structure of the grains. The BSE images show darker parts in the middle of the microcrystals and bright parts in the shell (higher average atomic number). BSE images further illustrate that the brightness of the shell of the microcrystals increases with increasing bromide concentration. Although according to the preparation of the microcrystals an homogeneous Ag(Cl,Br) shell should have been obtained, BSE image analysis points out that the heterogeneity of the bromide distribution increases with increasing bromide concentration in the shell; even at low bromide concentration not all Ag(Cl,Br) microcrystals have a homogeneous bromide distribution in their shell.

X-ray mapping was also applied to study the distributions of halides (Cl, Br and I) and other elements in various types silver halide microcrystals. For the microcrystals of multi-halide composition or indefinite thickness, TE image and BSE image cannot show the compositional outline, however, in spite of its poor resolution compared to TE and BSE images, X-ray mapping can do it under some conditions. Fig. 9 was acquired from a single tabular microcrystal for three elements and for the background (X-ray continuum radiation in a selected region). Image processing of elemental images was carried out to subtract the background and get maps of the ratio of two elements. The cubic microcrystals with epitaxial or conversion growths were studied in this way. For some cubic microcrystals and the cubic microcrystals with epitaxial growths outside their corners, after tilting at an angle of 35°, at least two faces of the cube were seen (Fig. 4). The SE and BSE images of the cubic microcrystal then display a distorted shape, the X-ray map also shows non-uniform brightness in the middle and at the side of the crystal, but we can still get an outline of the distributions of four elements including Br, Cl and Ag.

The halide distributions of the samples were confirmed by X-ray spot analysis. By finding a correlation between X-ray intensity and bromide concentration, X-ray analysis in the spot mode yielded semiquantitative results. The results of X-ray spot analysis of the Ag(Cl,Br) cubic microcrystals in Figures 7 and 8 are shown in Table 1. For the Ag(Cl,Br) cubic microcrystals with epitaxial growth inside the corners of the crystals, the Br/Ag concentration ratios are about 0.20 in the corner sections, 0.007 in the center and about 0.01 in the sides, this confirms the BSE analysis in Fig. 7 where the corners of the microcrystal (bright parts) were said to have high bromide contents. For the AgCl core-Ag(Cl,Br) shell microcrystals, the Br/Ag concentration ratio measured in the middle of the microcrystals is 0.16, this means that the penetration of the electron beam through the shell with 0.21 Br/Ag concentration ratio into the pure AgCl center, made the observed ratio of the middle lower than that of the shell. The bromide concentrations at the corners are a little higher than these at the sides. Three to four crystals of every sample are studied. The statistical results of these analyses have been summarized but cannot be discussed here. The X-ray spot analysis confirms the element non-specific information of the backscattered electron images and provides quantitative results on a relative scale.

Conclusions

Elemental distributions and contents of tabular and cubic silver halide microcrystals were determined by BSE imaging, STE imaging, X-ray mapping and X-ray analysis in the spot mode. The acquisition of backscattered electrons was improved by selection of the image processing system parameters. The mean atomic number contrast of processed BSE images corresponds with the elemental outline in some samples. X-ray maps also provided some indications of elemental distributions. X-ray analysis in the spot mode yielded semiquantitative results. The analytical results illustrate that various

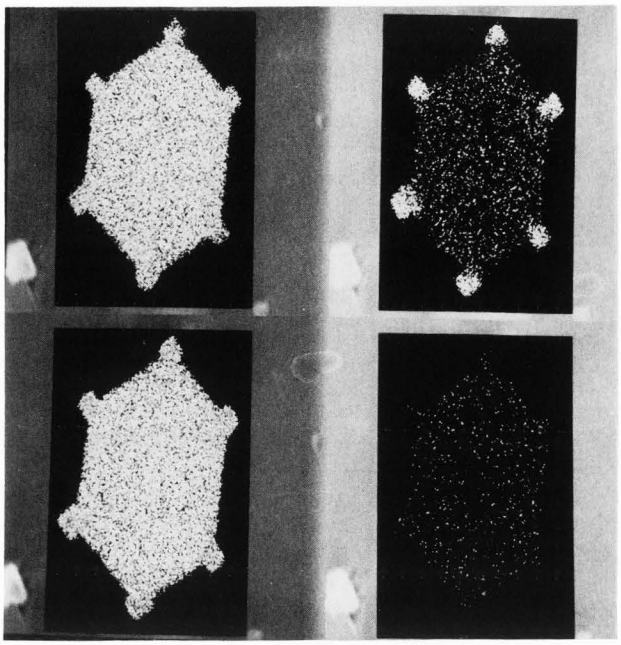

Figure 9. X-ray map of a tabular Ag(Br,I) microcrystal with AgCl epitaxial growths in the corners. Upper left: BrLα; upper right: ClKα; lower left: AgLα; lower right: background (4.65 to 4.95 keV). Crystal size = 2 μm.

epitaxial or conversion growths do or do not happen at different positions in different types of microcrystals.

This work indicates that the combination of the different analytical methods referred to above can be used to determine with good confidence the elemental distribution in silver halide microcrystals, particularly in the analysis of the cubic microcrystals whose shape and variable transparency after tilting make them difficult to analyze. The analyses also provide valuable information on the choice of the preparation conditions for silver halide microcrystals.

TABLE 1. X-ray spot analysis results for cubic microcrystal.

Crystal scheme & spot position	Spot	Br/Ag[a] sample 1[b]	Br/Ag sample 2[c]
1. 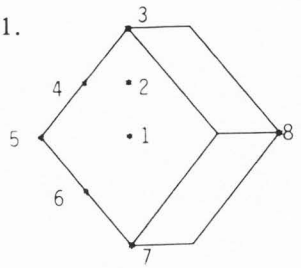 Size: 0.5 μm	1	0.007	0.161
	2	0.018	0.206
	3	0.168	0.236
	4	0.010	0.198
2. 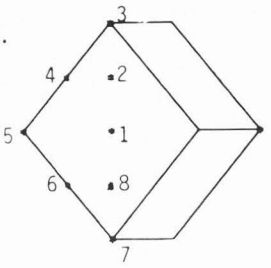 Size: 0.44 μm	5	0.239	0.215
	6	0.048	0.187
	7	0.136	0.223
	8	0.165	0.217

[a] Br/Ag is concentration ratio of Br to Ag.
[b] The microcrystal is shown in Fig. 7.
[c] The microcrystal is shown in Fig. 8.

Acknowledgments

We thank Prof. David C Joy, EM Facility, the University of Tennessee, U.S.A., for providing the Monte Carlo simulation programs used in this paper.

References

Archard G (1961) Back scattering of electrons. J. Appl. Phys. **32**, 1505-1509.

Everhart TE (1960) Simple theory concerning the reflection of electrons from solids. J. Appl. Phys. **31**, 1483-1490.

Gao XL, Gijbels R, Nys B, Jacob W, Gilliams Y (1989) A new and convenient method for the analysis of the halide distribution in tabular photographic silver halide microcrystals by backscattered electron imaging. J. Imaging Sci. **33**, 87-91.

Gijbels R, Van Puymbroeck J, Ketellapper LW (1987) Depth distribution of halide in silver halide emulsions by SIMS. In: Progress in Basic Principles of Image Systems, Granzer F, Moisar E (eds.), Vieweg F & Sohn, Braunschweig/Wiesbaden, Germany, 93-97.

Joy DC (1988) An introduction to Monte Carlo simulations. Inst. Phys. Conf. Ser. No. **93**, Vol. I. Inst. Physics, Bristol, U.K., 23-32.

Kelly TM, Mason MG (1976) Halide composition profile in silver halide microcrystals. J. Appl. Phys. **47**, 4721-4725.

King MA, Loretto MH, Maternaghan TJ, Berry FJ (1987) The investigation of iodide distribution by analytical electron microscopy. In: Progress in Basic Principles of Image Systems, Granzer F, Moisar E (eds.), Vieweg F & Sohn, Braunschweig/Wiesbaden, Germany, 73-79.

Maskasky J (1987) A enhanced understanding of silver halide tabular grain growth. Imaging Sci. **31**, 15-26.

Maternaghan TJ, Falder CJ, Levi-Setti R, Chabala JM (1990) Elemental mapping of silver halide emulsion microcrystals by high resolution imaging SIMS. J. Imaging Sci. **34**, 58-65.

Newbury DE, Yakowitz H (1976) Studies of the distribution of signals in the SEM/EPMA by Monte Carlo electron trajectory calculations. NBS Spec. Publ. (U.S.) No. **460**, National Bureau of Standards (now National Institute for Standards and Technology),

Gaithersburg, Maryland, U.S.A., 15-43.

Niedrig H (1978) Physical background of electron backscattering. Scanning **1**, 17-34.

Raeymaekers BJ, Liu X, Janssens KH, Van Espen PJ, Adams FC (1987) Determination of the thickness of flat particles by automated electron microprobe analysis. Anal. Chemistry **59**, 930-937.

Wu S, Van Daele A, Geuens I, Jacob W, Gijbels R, Verbeeck A, De Keyzer R (1990) Elemental mapping and analysis of silver halide microcrystals by STEM-EDX. In: The Advancement of Imaging Science & Technology, Peng B, Huang Y, Wang S, Qi Z (eds.), International Academic Publishers, Beijing, China, 65-69.

Discussion with Reviewers

J.D. Brown: How were the measured intensities converted to concentrations? Was a thin film or bulk calculation used?

Authors: Neither thin film nor bulk model was used. The quantification was based on the use of standards, i.e., microcrystals with known concentration. The measured intensities were converted into concentration after finding the correlation between the X-ray intensity ratios and the known concentration ratios. Homogeneous Ag(Cl,Br) samples with different bromide concentration (2% , 5%, 10%, 20%) were prepared as standard samples. For a specimen of given concentration, three microcrystals were selected. Eight different areas in each microcrystal were measured. A total of 24 measurements were carried out for every concentration. The results show satisfactory precision (relative standard deviation less than 20%). The counts were used in establishing the relationship between X-ray counts ratios and concentration ratios. A linear relationship was found.

J.D. Brown: In the Monte Carlo plots no backscattered electrons are seen in the trajectory and only one or two can be inferred in the X-ray generation plots even though the formulae for backscatter factor would suggest a few percent of electrons are backscattered. Can you comment on this discrepancy?

Authors: For beam broadening, we are more interested in obtaining a direct visual representation of the interaction in the silver halides, so a limited number of trajectories is more suitable to observe the primary electron beam broadening and therefore only 100 trajectories were selected. When statistically valid results are needed, a large number of trajectories would have to be calculated. According to the calculation with 1000 trajectories and at 80 keV incident energy, for 0.1 μm thickness AgBr or AgCl, the BSE yield is less than 1%; for 0.5 μm thickness AgBr or AgCl, the BSE yield is 2%. So the backscatter factor can be obtained from the calculation of a large number of trajectories, but hardly from 100 trajectories, as in Figures 1a and 2a.

R.H. Packwood: Please comment on the difference between epitaxial and conversion growth as it relates to silver halides.

Authors: These terms refer to two types of silver halide microcrystal growth. Epitaxial growth is obtained by adding silver ions and various halide ions on the original silver halide to form a new phase. Conversion is obtained by adding halide ions, which can replace the halide in the original microcrystals; a new silver halide phase of low solubility is formed.

K. Murata: If the thickness of the samples in Table 1 is, say 0.5 μm, electrons with oblique incidence can excite the corner where the Br/Ag concentration ratio is 0.239 as can be speculated from Fig. 2. But you have a concentration ratio of only 0.007 at position 1 in sample 1. Is the above effect so small or does bromide concentrate at the very surface layer?

Authors: The electron beam broadening can excite the corner at the bottom, so the selection of the analysis spot and the crystal orientation must take that factor into account. Fig. 4 shows two crystal orientations. In order to obtain statistically meaningful results, many microcrystals were measured in these two orientations; some measurements show, indeed, high Br in the center. Due to space limitation, it cannot be discussed here. If the center of the cube is of interest, another orientation (Fig. 4a) would show less influence from the corners at the bottom. Moreover, as shown in Fig. 7, the epitaxial growth of that microcrystal did not occur at every corner. It is, in fact, very difficult to prepare microcrystals with epitaxial growth at all corners.

K. Murata: Is it possible to do quantitative analysis with the signal of backscattered electrons, knowing elements composing a sample?

Authors: The backscattered electron signal not only depends on the composition of the crystal, but also on its thickness. Since the latter parameter is not constant, it will be difficult to quantify the BSE images, even for a binary system (2 halides). For more complicated cases (e.g., 3 halides) it is practically impossible. However, the BSE images are very useful to indicate the different phases within a crystal, which should be analyzed by X-ray microanalysis (element-specific information).

K. Murata: If you calculate the X-ray excitation volume with Monte Carlo simulation, including the boundary condition, you will be able to perform more accurate quantitative analysis, I suppose. Could you comment on this proposal?

Authors: We completely agree with you. The program of Monte Carlo simulation of X-ray generation was improved several times by Prof. Joy. If the boundary condition and the oblique incidence had been included, the program would have been more satisfactory.